# STOCHASTIC ACTIVATIONS

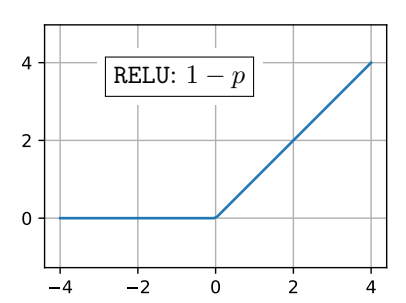
## Anonymous authors

Paper under double-blind review

## Abstract

We introduce stochastic activations. This novel strategy randomly selects between several non-linear functions in the feed-forward layer of a large language model. In particular, we choose between SILU or RELU depending on a Bernoulli draw. This strategy circumvents the optimization problem associated with RELU, namely, the constant shape for negative inputs that prevents the gradient flow. We leverage this strategy in two ways:

- (1) We use stochastic activations during pre-training and fine-tune the model with RELU, which is used at inference time to provide sparse latent vectors. This reduces the inference FLOPs and translates into a significant speedup in the CPU. Interestingly, this leads to much better results than training from scratch with the RELU activation function.
- (2) We evaluate stochastic activations for generation. This strategy performs reasonably well: it is only slightly inferior to the best deterministic non-linearity, namely SILU combined with temperature scaling. This offers an alternative to existing strategies by providing a controlled way to increase the diversity of the generated text.



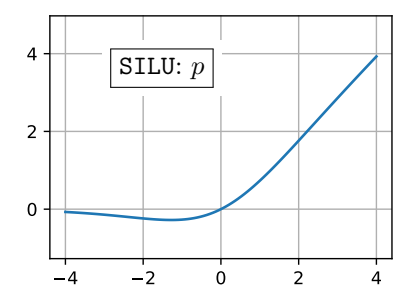


Figure 1: Stochastic activation randomly selects one of two activations when x < 0:
(1) RELU selected with probability 1 - p; otherwise (2) another activation, in particular SILU.

# 1 Introduction

Large language models (LLMs) (Devlin et al., 2019; Chowdhery et al., 2022; Brown et al., 2020; Vaswani et al., 2017) have revolutionized natural language processing, enabling unprecedented capabilities in text generation, comprehension, and reasoning. Their success stems from scaling model parameters and leveraging vast amounts of data, but this comes with a significant computational complexity. As the demand for more efficient and powerful models grows, researchers are increasingly focused on optimizing their training processes to balance performance with resource constraints.

The majority of the LLM parameters are in the Feed-Forward Network (FFN) layers, where they memorize the training data. FFNs are two linear layers separated by an *activation function*, and sometimes an additional linear layer that serves as a gating operation. The activation is a  $\mathbb{R} \to \mathbb{R}$  non-linear function. In this context, the choice of activation function plays a crucial role for both the model's expressivity and efficiency. The simplest activation is RELU (Rectified Linear Unit), that allows positive values to pass through and forces negative inputs to zero. RELU is *sparsity-inducing*, since, on average, half of its outputs

are zero (in practice significantly more). Within a two-layer Multilayer Perceptron, this means that inference on the second layer is a matrix-sparse vector multiplication, so it can be implemented with fewer FLOPs than a matrix-dense vector multiplication. Note that effectively improving the runtime with this sparsity pattern remains challenging.

In practice, the Sigmoid Linear Unit (SILU) activation, combined with a gated design, has consistently outperformed RELU in terms of model accuracy (Shazeer, 2020). Unfortunately, SILU does not induce sparsity. One plausible explanation for RELU's underperformance is that its gradient for negative input values is zero, which hinders optimization by preventing weight updates in a significant portion of the network. Solutions like Leaky RELU (Maas et al., 2013) circumvent this problem by ensuring non-zero gradient almost everywhere, but they are inferior to SILU and involve abandoning sparsity. In contrast, if the so-called "dying RELU problem" optimization challenge could be effectively addressed, RELU's theoretical advantages – such as sparsity and computational efficiency – may translate into performance comparable to SILU for a lower number of FLOPs. This disparity presents a challenge: how to harness the efficiency benefits of sparse activations, such as RELU, without sacrificing the empirical advantages of SILU. This motivates our exploration of alternative training strategies that mitigate RELU's limitations while preserving its benefits.

In this work, we consider two ways to approach this problem. The first approach is activation fine-tuning, denoted <code>Swi+FT</code>: we pre-train the model with an activation that facilitates efficient large language model optimization, then we change the activation to <code>RELU</code> and adapt the model by fine-tuning it further. Our second approach, referred to as <code>StochA</code> (stochastic activations), is a novel technique that randomly selects between multiple activations, either at train or test time. Both approaches allow models to benefit from the superior optimization properties of <code>SILU</code>. These hybrid strategies combine the best of both worlds – maintaining high model performance while unlocking the computational efficiency of sparse activations.

In summary, this paper makes the following contributions:

- We introduce and analyze two strategies that employ different activation functions at training and inference time, namely Swi+FT and StochA. Both are complementary and make it possible to use activations at inference time that differ from those employed during pre-training.
- We produce RELU-based models that are much better than those obtained with regular training, i.e., our methods significantly outperform training with RELU only.
- We show that stochastic activations, when used at inference time, provides an alternative way to generate diverse sequences compared to traditional temperature sampling or other variants.

## 2 RELATED WORK

Standard activation functions Activations are at the core of deep learning, in that they are needed to depart from defining a linear function with limited expressivity. While early neural network architectures were inspired by logistic regression, such as sigmoidal and tanh activations, many activation functions have been evaluated for the Feed Forward layers (FFNs) of transformers. Vaswani et al. (2017) used RELU (Glorot et al., 2011). However, using the RELU activation function leads to some neurons getting stuck in the negative region. As a consequence, they stop learning entirely, since the gradient is zero for negative inputs, and their weights do not get updated. In contrast, Touvron et al. (2023) used SILU as the activation function for the FFN layers of the transformer for the first Llama models. Shazeer (2020) discusses the benefits of SWIGLU, which consists of SILU with gating. There exist many other activation functions such as the Gaussian Error Linear Unit (GELU) (Hendrycks & Gimpel, 2016), Scaled Exponential Linear Unit (SELU) (Klambauer et al., 2017), Swish (Ramachandran et al., 2018) and gated SILU, among others.

In particular, the Leaky RELU (Maas et al., 2013; Redmon et al., 2015; Ridnik et al., 2021; Guo et al., 2024) tried tackling the dying RELU problem by allowing a small, non-zero gradient when the input is negative in order to keep the neurons active and the gradients flowing, reducing the risk of dead neurons.

Adaptive activation functions Lee et al. (2022) propose an activation, called Adaptive Swish (ASH), that uses stochastic sampling of the top-k percentile elements. It is a generalization of the Swish (Ramachandran et al., 2018) activation function, that uses adaptive thresholding and selects only the values in the top percentiles and sets these to zero otherwise. The threshold is not fixed but depends on the distribution of the input making it an example of a stochastic activation.

**Dropout and structured Dropout variants** In the original dropout paper (Srivastava et al., 2014), the authors propose a regularization technique to reduce overfitting and improve generalization of a neural network. It consists of setting to zero a subset of neurons at each training step. Consequently, the dropped neurons do not contribute to the forward pass or receive weight updates during back-propagation. At inference time, all neurons are used and their outputs are scaled by the dropout probability.

LayerDrop (Fan et al., 2019) randomly drops entire layers during training, hence, it encourages the model to be robust to missing layers. At inference time, some layers can be pruned, trading off between speed and accuracy as needed. While the method does not make the model sparse in the usual sense, it induces structured sparsity in the computation graph during training. Other works also introduce structured dropout variants such as DropBlock (Ghiasi et al., 2018), Bayesian dropout (Gal & Ghahramani, 2016), or Beit (Bao et al., 2021) and masked-autoencoder (He et al., 2022) in computer vision, among others.

Quantization approaches Fan et al. (2020) propose Quant-noise, that mimicks quantization during training by introducing noise to a random subset of weights for each forward pass enabling high compression ratios while maintaining the original model performance. It uses the Straight-Through estimator (STE) (Bengio et al., 2013; Hinton, 2012) to compute the gradients. This training technique ensures that the model is pretrained to observe both the train-time (unquantized) and the inference-time (quantized) models. This ensures proper optimization, bypassing the flat gradient caused by quantization and reducing the discrepancy that results from the late quantization of the model weights.

Sparsity by design Some works propose to enable sparsity directly in the architecture, for instance, the Mixture of Experts (MoE) or the Product-Key Memory (PKM). The PKM architecture (Lample et al., 2019) uses a memory layer for neural networks which enables the model to access a large learnable memory and thus, it enables long term memory capabilities. It leverages product quantization (PQ) (Jégou et al., 2011) by splitting the key in two parts and using each part in separate codebooks. The combination of each PQ index enables the model to access a larger memory space efficiently. At each forward pass, only a small subset of the memory is accessed, making it computationally efficient. [H: Cite recent works built upon this: bytedance, Google and Meta/MCU]

Mixture of Expert (MoE) models (Yang et al., 2024; Wei et al., 2024; DeepSeek-AI et al., 2024; Jiang et al., 2024) dynamically select and activate the relevant subset of parameters based on the characteristics of the input data. The MoE approach allows MoE models to expand their capacity without proportionally increasing computational complexity. See Mu & Lin (2025) for an overview of the MoE and references therein.

### 3 Using different activations at train and test time

This section introduces two strategies for improving the optimization during pretraining using an optimization-compliant activation, while preparing the model to a potentially different activation at test time. First we introduce the Swi+FT fine-tuning approach. Then we introduce our Stochastic Activation Stocha.

### 3.1 Fine-tuning with Relu: Swi+FT

In the following, we use SILU and RELU as our training and inference activations. For reference, they are defined in  $\mathbb{R} \to \mathbb{R}$  as:

$$RELU(x) = \max(x, 0) \qquad SILU(x) = x\sigma(x), \tag{1}$$

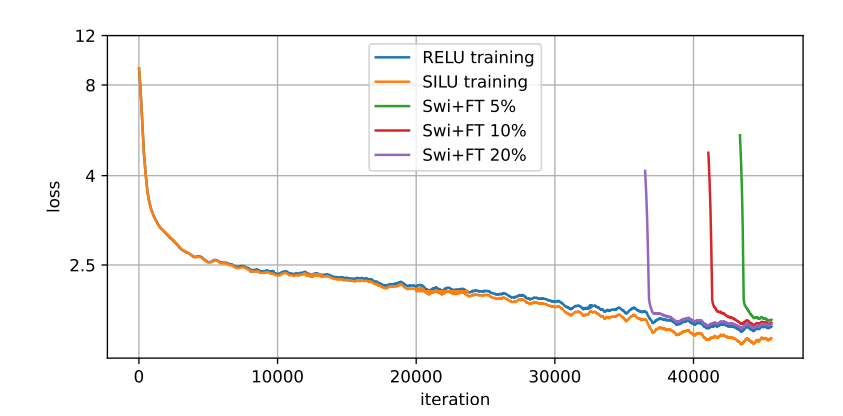


Figure 2: Swi+FT: Training loss. Most of the training is carried out with SILU, with  $\alpha=5\%$ , 10% and 20% of the final steps using RELU. Note the loss spike when we switch the activation. The model rapidly recovers and converges to a regime where RELU is performing well while providing sparsity. This strategy needs to be combined with StochA to provide good models operating with RELU.

where  $\sigma(x) = 1/(1 + \exp(-x))$  is the sigmoid function. We choose these two activations because SILU is one of the best options in terms of accuracy, while RELU is simple and sparse. The two activations are also similar: same asymptotes at  $-\infty$  and  $+\infty$ , and the same value at 0. SILU is differentiable twice (unlike RELU) and, interestingly, non-monotonous.

In our proposed approach, the training operates as follows:

- Most of the training steps (during a proportion  $1 \alpha$  of the total number of iterations) are carried out with a first activation that is deemed preferable for training. We typically employ SILU for this stage.
- We then switch the activation to that used for inference for the rest of the training.

We mostly set  $\alpha=0.05$  or  $\alpha=0.1$ , which mean that only 5% or 10% of the training steps are carried out using the inference-time activation. We do not re-initialize the parameters of the optimizer when switching between activations, and similarly we do not use any warm-up. This does not disrupt the optimization because the SILU and RELU activations are relatively similar. We observe a spike in the loss at the time we change the activation, see Figure 2. However, the optimization rapidly recovers. In practice, the fine-tuning replaces the last iterations of the pretraining. The learning rate follows a cosine schedule which gradually reduces it to  $1/100^{\rm th}$  of its peak value. Therefore, at 5% or 10% of the end of the training, the learning rate is already  $60\times$  or  $29\times$  lower than its peak, which is compatible with a fine-tuning regime.

### 3.2 STOCHASTIC ACTIVATION: STOCHA

A stochastic function, parametrized by a random variable  $\omega$ , is a function

$$y = \Psi(x, \omega) \tag{2}$$

that maps inputs  $x \in \mathbb{R}$  to output  $y \in \mathbb{R}$  with randomness involved. The dependence on  $\omega$  emphasizes that the outcome depends on an underlying probability space. In that sense, the function  $\Psi(\cdot,\omega)$  is deterministic for each realization of  $\omega$ , but is stochastic overall. In particular, we consider the case depicted in Figure 1, where  $\omega \sim \text{Bernoulli}(p)$  is a binary random variable parametrized by a parameter p:  $\omega \in \{0,1\}$  such that  $\mathbb{P}(\omega=1)=p$  and  $\mathbb{P}(\omega=0)=1-p$ . In that case, the stochastic function  $\Psi_p(\cdot)$  is defined such that

if 
$$x < 0$$
,  $\Psi_p(x) = (1 - \omega) \times \text{RELU}(x) + \omega \times \text{SILU}(x)$ , (3)

which amounts to randomly selecting between the RELU and SILU activations for x < 0. If  $x \ge 0$  we choose either  $\Psi_p(x) = x$  or  $\Psi_p(x) = \text{SILU}(x)$ , see the baseline paragraph below.

This strategy ensures that the network is compatible with two regimes. The first one, drawn with probability 1-p, is the inference-time mode, where we prepare the network to employ RELU during generation, in order to exhibit sparsity. The second mode aims to facilitate optimization during training. The choice of the SILU activation is motivated by the regular deterministic gated design by (Shazeer, 2020) adopted by most state-of-the-art LLMs.

**Notation** To specify an activation, we separately define the function for the positive and negative range of inputs. For example R-S+ means that RELU is used for the negative range and SILU for the positive. When StochA is used, we indicate [S|R]-S+, which means that for the negative range, we sample SILU with probability p and RELU with probability 1-p.

Baselines The two natural baselines are the deterministic functions SILU and RELU. We also introduce two non-stochastic baselines in order to disentangle the effect that could come from combining SILU and RELU separately in the positive and negative domain: these baselines are denoted by S-R+ and S-R+.

	x < 0	$x \ge 0$
RELU	0	x
SILU	$x \cdot \sigma(x)$	$x \cdot \sigma(x)$
R-S+	0	$x \cdot \sigma(x)$
R+S-	$x \cdot \sigma(x)$	x

Discussion The stochastic strategy resembles activation dropout (Srivastava et al., 2014), which can be regarded as a particular case of our method where one of the activations is the null function. However, the objective of dropout is to avoid overfitting. Our motivation is closer to Quantization-aware training (Jacob et al., 2017), more specifically, to the QuantNoise strategy of Fan et al. (2020), where the model is pretrained to observe both the train-time (unquantized) and the inference-time (quantized) models. In QuantNoise, using these two modes during training time ensure both the proper optimization, without suffering the flat gradient inherent to quantization, while reducing the discrepancy that results from the late-quantization of the model weights.

Alternative construction of a stochastic activation. An alternative construction is to randomly select between the identity function  $x \mapsto x$  and the constant zero function  $x \mapsto 0$  with a sigmoidal probability  $\sigma(x)$ . As a result, in expectation this function is given by

$$\mathbb{E}[\operatorname{sa}(\mathbf{x})] = (1 - \sigma(x)) \cdot 0 + \sigma(x) \cdot x = \sigma(x) \cdot x,\tag{4}$$

where we recognize the SILU(x) function. While the simplicity of this construction is mathematically appealing, our preliminary experiments revealed that it does not work very well.

### 3.3 Inference-time strategies and evaluation

At test time, we evaluate and analyze models trained with Swi+FT and/or StochA as follows:

**RELU at test time.** This is how we can enable sparsity. The corresponding evaluations therefore measure the performance on benchmarks when using this activation at test time.

**Exploiting sparsity** On an input  $x \in \mathbb{R}^D$ , the gated FFN computes:

$$y = W_2 \times (\text{RELU}(W_1 \times x) \odot (W_3 \times x)) \text{ with } W_1, W_3 \in \mathbb{R}^{N \times D} \text{ and } W_2 \in \mathbb{R}^{D \times N},$$
 (5)

assuming column vectors and noting  $\odot$  the element-wise multiplication. When the activation RELU( $W_1 \times x$ ) has a fraction s of zeros, the multiplications by  $W_2$  and  $W_3$  can exploit this sparsity: the baseline of 3ND FLOPS reduces to (3-2s)ND.

Note that exploiting the sparsity to increase the computational throughput is not straightforward. At training time, the runtime is dominated by matrix-matrix multiplications, where even a 90% sparsity rate is not guaranteed to yield efficiency gains. At inference time with one prompt at a time, the bottleneck is the memory access used during matrix-vector multiplications. When  $W_2$  is stored by rows and  $W_3$  by columns, the sparsity can be exploited to avoid a fraction s of the memory reads, that are contiguous. This implementation nearly yields the expected speedup (see experimental section).

**Stochastic activation at test time.** The following only applies to the StochA strategy: we evaluate the performance when if leverage the randomness at test time, i.e., in this case, we do not use RELU. This choice has two interests:

- 1. To quantify the effect of the activation discrepancy between train and test.
- 2. To generate multiple outputs from the same prompt with the randomness of StochA.

For the second usage, the standard way to generate multiple outputs from the same prompt is to replace the greedy decoding with a random sampling of the token from its probability distribution. This sampling can be tuned by setting a softmax temperature T which adjusts between completely uniform sampling  $(T \to \infty)$  and strict maximum sampling  $(T \to 0)$ . In both cases, we keep the one generated output with the highest normalized log likelihoods, *i.e.*, the per-token average log-likelihood, as predicted by the model.

### 4 Experiments with large language models

### 4.1 Experimental setting

**Model architecture** We train dense decoder-only models. The transformer blocks use grouped-query attention (Ainslie et al., 2023). These models use RMSNorm (Zhang & Sennrich, 2019) with prenormalization, rotary positional positional encoding (RoPE) (Su et al., 2021) with  $\theta = 500000$  and train with document causal masking. We use the SILU activation (Shazeer, 2020) for the SILU baseline. The structure of our LM1.5B and LM3B models is detailed in Table 4 in Appendix A.

**Training hyper-parameters** We train the models with AdamW optimizer (Loshchilov & Hutter, 2017) with  $\beta_1 = 0.9$ ,  $\beta_2 = 0.95$ , learning rate of  $lr = 3 \times 10^{-3}$ , weight decay of 0.1, and gradient clipping at norm 1.0. After 2000 steps of linear warm-up, we use a cosine decay learning rate schedule with peak learning rate  $8 \times 10^{-4}$  and decay by a factor of 1/100 over the training horizon.

**Tokenizer** We use the Llama3 (Dubey et al., 2024) tokenizer, which is a fast Byte-Pair Encoding tokenizer implemented with TikToken.2 The vocabulary contains 128 000 regular tokens as well as 256 reserved tokens.

**Pre-training** We pre-train the LM1.5B and LM3B models with 47B and 80B tokens, respectively, from a diverse collection of mostly English natural language and coding data. We use a batch size of 1M tokens and a context length of 8192 tokens.

Evaluation Benchmarks We employ two types of benchmarks for zero or few-shot evaluation, which we describe in more detail in Appendix C and Table 6. The first type is code generation tasks: HumanEval+ (Liu et al., 2023) and MBPP (Chen et al., 2021). The second type consists of common sense and general reasoning: HellaSWAG(Zellers et al., 2019), ARC(Clark et al., 2018), PIQA (Bisk et al., 2020), OBQA (Mihaylov et al., 2018), WinoGrande (Sakaguchi et al., 2020), NQ (Kwiatkowski et al., 2019), RACE (Lai et al., 2017), TQA (Joshi et al., 2017) and GSM8K (Cobbe et al., 2021).

### 4.2 PERFORMANCE ANALYSIS OF SWI+FT AND STOCHA WITH RELU AT INFERENCE TIME

In this section we analyze the effect of our proposal when using RELU at test time. In Appendix B, we provide a complementary analysis of the sparsity. Depending on the setting, the average rate of 0s can be higher than 90%, when using the RELU at test time.

Cross-entropy performance. Table 1 provides the impact on the training and validation losses of multiple choices with the LM1.5B and LM3B models. We observe that the training loss using stochastic activation at train time is lower than that obtained with

		aining a	ctivation $x > 0$	p		train	LM1.5E	s val	train	LM3B val	val
Activation	p	1-p			Swi+FT		RELU	StochA	İ	RELU	StochA
SILU	SI	LU	SILU	-	Х	2.105	2.122*		1.966	1.974*	
RELU	RE	LU	RELU	-	X	2.140	2.161		2.027	2.043	
S-R+	SI	LU	RELU	-	X	2.101	$2.124^{\star}$		1.970	$1.980^{\star}$	
R-S+	RE	LU	SILU	-	X	2.123	$2.151^*$		2.016	$2.033^{\star}$	
[S R]-R+	SILU	RELU	RELU	0.3	×	2.120	2.363	2.146	1.993	2.257	2.006
[S R]-R+	SILU	RELU	RELU	0.5	X	2.120	2.507	2.145	1.990	2.889	1.999
[S R]-S+	SILU	RELU	SILU	0.3	X	2.115	2.305	2.143	1.987	2.257	1.996
[S R]-S+	SILU	RELU	SILU	0.5	X	2.115	2.530	2.143	1.984	2.753	1.995
[S R]-R+	SILU	RELU	RELU	0.3	✓	2.123	2.141	2.251	1.988	1.998	2.177
[S R]-R+	SILU	RELU	RELU	0.5	✓	2.129	2.148	2.307	1.989	2.002	2.306
[S R]-S+	SILU	RELU	SILU	0.3	✓	2.120	2.138	2.221	1.982	1.992	2.103
[S R]-S+	SILU	RELU	SILU	0.5	✓	2.125	2.144	2.301	1.985	1.994	2.234

Table 1: Losses: train is computed over the last 500 steps of the training loss of LM1.5B, val is measured after training on a different set set of text and code using the RELU activation\* or StochA, i.e., the same activation used at train time (possibly deterministic). If Swi+FT is enabled, we switch to RELU for the last 5% steps. \*: for the deterministic baselines SILU, S-R+ and S+R-, we do the inference with the same activation used at train-time (not RELU).

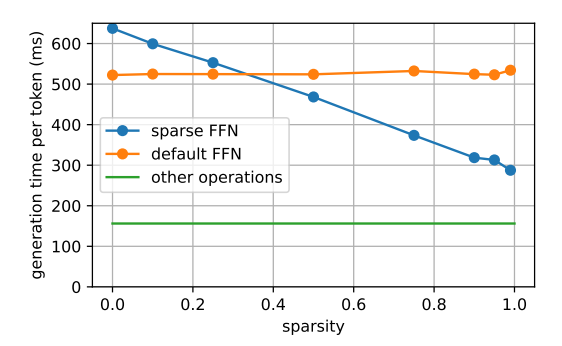


Figure 3: Total inference time for 1 token on CPU, as a function of the activation sparsity, with a LM3B model trained with Swi+FT. The "other operations" include the attention layers (they are not dominant because the generation is limited to 200 tokens), the normalization and the execution overheads. At 90% sparsity the speedup is  $\times 1.65$ . The timings are measured on a single core of a Xeon 8462Y+ machine.

RELU. However the validation entropy is not competitive per se, due to the remaining train-inference discrepancy of activation. This is solved by Swi+FT: switching to the RELU activation function and fine-tuning for the last 5% or 10% steps percentage of the training steps drastically boosts the test-time inference. These results outperform the results obtained with regular RELU training, while using the same activation at test time.

Fast inference with RELU sparsity The activation sparsity can be exploited to avoid fetching 90% of the matrices  $W_1$  and  $W_3$  of the FFN (see Eq. 5 ands detailled sparsity rate in Appendix B). This has a direct benefit on CPU, see Figure 3: the 90% sparsity provides a 65% speedup. On GPU the additional challenge is to make the computation sufficiently predictable to balance the load between CUDA threads.

Complementary of StochA and Swi+FT with RELU finetuning Figure 4 shows the training loss when using StochA and Swi+FT jointly. When switching the activation to RELU, we observe a spike in the loss, but the optimization rapidly recovers, and then converges to a model having a better performance than the one produced when training with RELU from scratch. In contrast, in the case where we employ Swi+FT alone (Figure 2), fine-tuning with RELU after pretraining with SILU is not enough to obtain performance improvements. This shows that both approaches are complementary.

The impact of  $\alpha$  can also be seen in Figure 4, where we compare the final loss reported for different fine-tuning values. In that case, setting  $\alpha=0.1$  is a good trade-off since the corresponding loss is lower than the RELU loss.

$\downarrow$ Benchmark/metric			LM1.5B				LM3B	
$\begin{array}{c} \text{train activation} \rightarrow \\ \text{inference activation} \rightarrow \end{array}$	base SILU SILU	lines RELU RELU	(a) Swi+FT [S R]-S+ RELU	(b) StochA [S R]-S+ [S R]-S+	base SILU SILU	elines RELU RELU	(a) Swi+FT [S R]-S+ RELU	(b) StochA [S R]-S+ [S R]-S+
hellaswag/acc_char winogrande/acc_char arc_easy/acc_char arc_challenge/acc_char piqa/acc_char obqa/acc_char race.middle/acc_char race.high/acc_char human_eval_plus/pass@1 mbpp/compiles@1 tqa/f1 nq/f1	0.585 0.593 0.568 0.313 0.732 0.346 0.518 0.382 0.073 0.978 0.243 0.123	0.561 0.571 0.562 0.286 0.720 0.340 0.516 0.379 0.067 0.970 0.217 0.107	0.574 0.568 0.600 0.331 0.724 0.378 0.509 0.372 0.049 0.960 0.229 0.121	0.576 0.568 0.562 0.314 0.720 0.340 0.498 0.375 0.055 0.980 0.232 0.113	0.684 0.657 0.675 0.390 0.767 0.390 0.565 0.414 0.128 0.992 0.351 0.169	0.633 0.615 0.642 0.348 0.751 0.380 0.538 0.402 0.110 0.980 0.293 0.146	0.630 0.679 0.396 0.765 0.384 0.559 0.407 0.128	0.678 0.620 0.671 0.376 0.761 0.408 0.549 0.416 0.116 0.982 0.342 0.145
average performance	0.123	0.107	0.121	0.113	0.109	0.146	0.170	0.145

Table 2: Performance per benchmark of the RELU and SILU (a) baselines for LM1.5B and LM3B compared to (b) models with StochA and Swi+FT at train time and RELU at test time, and (c) models with StochA at train and test time. We use the model with the best perplexity on val namely  $p=0.3, \alpha=0.05$  for Swi+FT and p=0.5 for StochA.

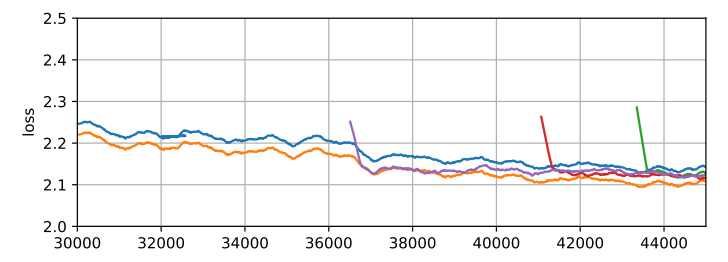
### 4.3 Performance on downstream tasks

Detailed results per benchmark Table 2 reports the results for the standard code generation, common sense and general reasoning benchmarks detailed in Appendix C. We consider multiple StochA models using few-shot or zero shot prompting, see Table 6 in the appendix for more details for each case. Observe first that the model with SILU is significantly better that a regular model with RELU. However, our models trained with StochA are slightly better or on par with SILU: either the model fine-tuned with Swi+FT and using RELU at inference time, or even the model that uses StochA at test time.

Performance when varying  $\alpha$  with Swi+FT. Figure 5 showcases that we can slightly surpass the SILU baseline if we first use a stochastic activation function during the LM1.5B model training and then switch to the RELU activation function for the last  $\alpha\%$  of the training steps, for  $\alpha \in \{5\%, 10\%, 20\%\}$ . The best performance is typically obtained with  $\alpha = 5\%$  or  $\alpha = 10\%$  for the LM1.5B model.

### 4.4 EXPLOITING STOCHA AT TEST TIME

Effectiveness of StochA a test time. In Table 1, in addition to the results with RELU at test time, we also report the train and validation losses obtained when employing StochA at test time. We observe that (1) using stochastic activations for inference works surprisingly well in spite of the randomness. The results are between RELU and SILU in most configurations; (2) When using StochA at test time, there is no need to fine-tune the model



	fiı	final loss					
$\alpha$	train	val (RELU)					
0	2.115	2.530					
0.05	2.125	2.144					
0.10	2.119	2.145					
0.20	2.126	2.155					

Figure 4: Training loss with Swi+FT and StochA: [S|R]-S+ activation with p=0.5 for  $\alpha=5\%$ , 10% and 20%, relative to RELU and SILU. Note that this plot this is zoomed in relative to Figure 2.

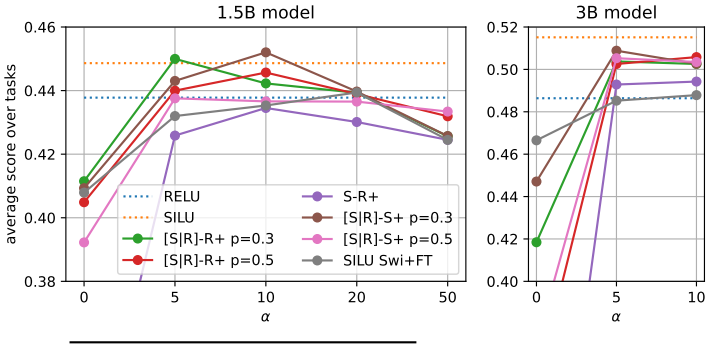
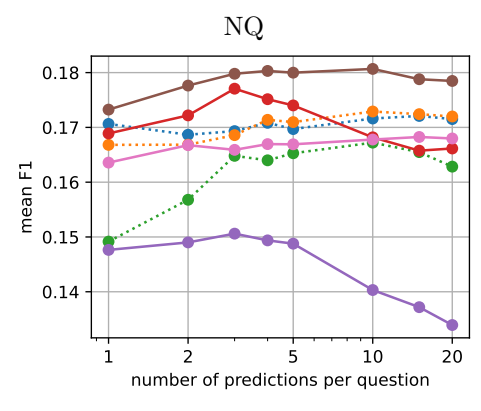


Figure 5: Swi+FT: analysis of the fine-tuning rate  $\alpha$ . We plot the average performance over the benchmarks as we vary the percentage  $\alpha$  of steps for which we switch to the RELU activation at the end of training. We use RELU at inference time.

p	LM1.5B		LM3B
0 (R-S+)	0.215	ī	0.222
0.3	0.443		0.504
0.5	0.426		0.505
0.7	0.453		0.495
1.0 (SILU)	0.454		0.515

Table 3: StochA: Impact on benchmarks performance (avg) as a function of the StochA p for [S|R]-S+ used at test time. The case p=0 corresponds to R-S+ while p=1 corresponds to the baseline SILU. The performance increases with more SILU in the mix. However, the stochasticity can be used to increase the generation diversity.



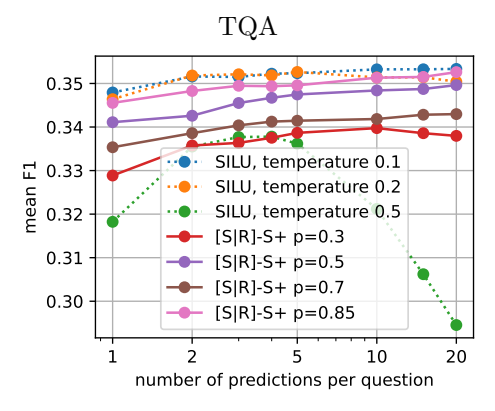


Figure 6: Comparison of ways to generate diverse responses in Q&A benchmarks: by varying the softmax temperature or by varying the [S|R]-S+p. The multiple generations are scored by normalized log likelihoods and the best generation is evaluated with an F1 score (y-axis).

with Swi+FT. This is expected since this strategy is intended to decrease the discrepancy with the test-time activation choice. Table 3 shows that the average benchmark performance generally increases when the stochastic mix approaches SILU. Therefore, StochA is primarily useful as a way to generate multiple outputs for the same prompt.

Diversity of generations ablations. Figure 6 shows how stochastic generation compares to temperature sampling to generate diverse outputs, see Section D for examples. We plot these on TQA and NQ, whose results are least noisy. For the best settings, the curves are increasing, which means that (1) the generations are indeed diverse and (2) that the normalized log likelihoods are a suitable scoring function. The StochA activations yield a higher performance than vanilla temperature sampling on NQ but are sub-par for TQA.

### 5 Conclusion

This paper has introduced a novel stochastic activation that preserves the performance of a non-sparse activation, such as SILU, while better adjusting to the behavior of a sparse one, such as RELU, at test time. This improves the inference times for the FFN layers of a transformer, translating into a speedup of typically  $\times 1.65$  for the FFN processing on CPUs while almost preserving the accuracy of the non-sparse SILU activation. Finally, we explore how stochastic activations can be leveraged at test time to improve diversity in model generations.

### REFERENCES

- Joshua Ainslie, James Lee-Thorp, Michiel de Jong, Yury Zemlyanskiy, Federico Lebron, and Sumit Sanghai. GQA: Training generalized multi-query transformer models from multi-head checkpoints. In Houda Bouamor, Juan Pino, and Kalika Bali (eds.), *Proceedings of the 2023 Conference on Empirical Methods in Natural Language Processing*, pp. 4895–4901, Singapore, December 2023. Association for Computational Linguistics. doi: 10. 18653/v1/2023.emnlp-main.298. URL https://aclanthology.org/2023.emnlp-main.298/.
- Jacob Austin, Augustus Odena, Maxwell Nye, Maarten Bosma, Henryk Michalewski, David Dohan, Ellen Jiang, Carrie J. Cai, Michael Terry, Quoc V. Le, and Charles Sutton. Program synthesis with large language models. ArXiv, abs/2108.07732, 2021. URL https://api.semanticscholar.org/CorpusID:237142385.
- Hangbo Bao, Li Dong, and Furu Wei. Beit: Bert pre-training of image transformers. ArXiv, abs/2106.08254, 2021. URL https://api.semanticscholar.org/CorpusID:235436185.
- Yoshua Bengio, Nicholas Léonard, and Aaron C. Courville. Estimating or propagating gradients through stochastic neurons for conditional computation. *ArXiv*, abs/1308.3432, 2013. URL https://api.semanticscholar.org/CorpusID:18406556.
- Yonatan Bisk, Rowan Zellers, Ronan Le bras, Jianfeng Gao, and Yejin Choi. Piqa: Reasoning about physical commonsense in natural language. *Proceedings of the AAAI Conference on Artificial Intelligence*, 34(05):7432-7439, Apr. 2020. doi: 10.1609/aaai.v34i05.6239. URL https://ojs.aaai.org/index.php/AAAI/article/view/6239.
- Tom B Brown, Benjamin Mann, Nick Ryder, Melanie Subbiah, Jared Kaplan, Prafulla Dhariwal, Arvind Neelakantan, Pranav Shyam, Girish Sastry, Amanda Askell, et al. Language models are few-shot learners. arXiv preprint arXiv:2005.14165, 2020.
- Mark Chen, Jerry Tworek, Heewoo Jun, Qiming Yuan, Henrique Ponde de Oliveira Pinto, Jared Kaplan, and OpenAI team. Evaluating large language models trained on code. 2021.
- Aakanksha Chowdhery, Sharan Narang, Jacob Devlin, and Google team. Palm: Scaling language modeling with pathways, 2022. URL https://arxiv.org/abs/2204.02311.
- Peter Clark, Isaac Cowhey, Oren Etzioni, Tushar Khot, Ashish Sabharwal, Carissa Schoenick, and Oyvind Tafjord. Think you have solved question answering? try arc, the ai2 reasoning challenge. ArXiv, abs/1803.05457, 2018. URL https://api.semanticscholar.org/CorpusID:3922816.
- Karl Cobbe, Vineet Kosaraju, Mo Bavarian, Mark Chen, Heewoo Jun, Lukasz Kaiser, Matthias Plappert, Jerry Tworek, Jacob Hilton, Reiichiro Nakano, Christopher Hesse, and John Schulman. Training verifiers to solve math word problems. *ArXiv*, abs/2110.14168, 2021. URL https://api.semanticscholar.org/CorpusID:239998651.
- DeepSeek-AI, Aixin Liu, Bei Feng, Bin Wang, Bingxuan Wang, Bo Liu, Chenggang Zhao, Chengqi Dengr, Chong Ruan, Damai Dai, Daya Guo, et al. Deepseek-v2: A strong, economical, and efficient mixture-of-experts language model, 2024. URL https://arxiv.org/abs/2405.04434.
- Jacob Devlin, Ming-Wei Chang, Kenton Lee, and Kristina Toutanova. Bert: Pre-training of deep bidirectional transformers for language understanding, 2019. URL https://arxiv.org/abs/1810.04805.
- Abhimanyu Dubey, Abhinav Jauhri, Abhinav Pandey, Abhishek Kadian, Ahmad Al-Dahle, Aiesha Letman, Akhil Mathur, Alan Schelten, Amy Yang, Angela Fan, et al. The llama 3 herd of models, 2024. URL https://arxiv.org/abs/2407.21783.
- Angela Fan, Edouard Grave, and Armand Joulin. Reducing transformer depth on demand with structured dropout. arXiv preprint arXiv:1909.11556, 2019.

Angela Fan, Pierre Stock, Benjamin Graham, Edouard Grave, Rémi Gribonval, Herve Jegou, and Armand Joulin. Training with quantization noise for extreme model compression. arXiv preprint arXiv:2004.07320, 2020.

- Yarin Gal and Zoubin Ghahramani. Dropout as a bayesian approximation: representing model uncertainty in deep learning. In *Proceedings of the 33rd International Conference on International Conference on Machine Learning Volume 48*, ICML'16, pp. 1050–1059. JMLR.org, 2016.
- Golnaz Ghiasi, Tsung-Yi Lin, and Quoc V. Le. Dropblock: A regularization method for convolutional networks, 2018. URL https://arxiv.org/abs/1810.12890.
- Xavier Glorot, Antoine Bordes, and Yoshua Bengio. Deep sparse rectifier neural networks. In *Proceedings of the fourteenth international conference on artificial intelligence and statistics*, pp. 315–323. JMLR Workshop and Conference Proceedings, 2011.
- Yinglong Guo, Shaohan Li, and Gilad Lerman. The effect of leaky relus on the training and generalization of overparameterized networks. *CoRR*, abs/2402.11942, 2024. doi: 10.48550/ARXIV.2402.11942. URL https://doi.org/10.48550/arXiv.2402.11942.
- Kaiming He, Xinlei Chen, Saining Xie, Yanghao Li, Piotr Dollár, and Ross Girshick. Masked autoencoders are scalable vision learners. In 2022 IEEE/CVF Conference on Computer Vision and Pattern Recognition (CVPR), pp. 15979–15988, 2022. doi: 10.1109/CVPR52688.2022.01553.
- Dan Hendrycks and Kevin Gimpel. Gaussian error linear units (gelus). arXiv: Learning, 2016. URL https://api.semanticscholar.org/CorpusID:125617073.
- Geoffrey Hinton. Neural networks for machine learning. Coursera, video lectures, 2012. Online course.
- Benoit Jacob, Skirmantas Kligys, Bo Chen, Menglong Zhu, Matthew Tang, Andrew G. Howard, Hartwig Adam, and Dmitry Kalenichenko. Quantization and training of neural networks for efficient integer-arithmetic-only inference. 2018 IEEE/CVF Conference on Computer Vision and Pattern Recognition, pp. 2704–2713, 2017. URL https://api.semanticscholar.org/CorpusID:39867659.
- Albert Q. Jiang, Alexandre Sablayrolles, Antoine Roux, Arthur Mensch, Blanche Savary, Chris Bamford, Devendra Singh Chaplot, Diego de Las Casas, Emma Bou Hanna, Florian Bressand, Gianna Lengyel, Guillaume Bour, Guillaume Lample, Lélio Renard Lavaud, Lucile Saulnier, Marie-Anne Lachaux, Pierre Stock, Sandeep Subramanian, Sophia Yang, Szymon Antoniak, Teven Le Scao, Théophile Gervet, Thibaut Lavril, Thomas Wang, Timothée Lacroix, and William El Sayed. Mixtral of experts. ArXiv, abs/2401.04088, 2024. URL https://api.semanticscholar.org/CorpusID:266844877.
- Mandar Joshi, Eunsol Choi, Daniel Weld, and Luke Zettlemoyer. Triviaqa: A large scale distantly supervised challenge dataset for reading comprehension. 05 2017. doi: 10.48550/arXiv.1705.03551.
- Herve Jégou, Matthijs Douze, and Cordelia Schmid. Product quantization for nearest neighbor search. *IEEE Transactions on Pattern Analysis and Machine Intelligence*, 33(1): 117–128, 2011. doi: 10.1109/TPAMI.2010.57.
- Günter Klambauer, Thomas Unterthiner, Andreas Mayr, and Sepp Hochreiter. Self-normalizing neural networks. In *Neural Information Processing Systems*, 2017. URL https://api.semanticscholar.org/CorpusID:13713980.
- Tom Kwiatkowski, Jennimaria Palomaki, Olivia Redfield, Michael Collins, Ankur Parikh, Chris Alberti, Danielle Epstein, Illia Polosukhin, Jacob Devlin, Kenton Lee, Kristina Toutanova, Llion Jones, Matthew Kelcey, Ming-Wei Chang, Andrew M. Dai, Jakob Uszkoreit, Quoc Le, and Slav Petrov. Natural questions: A benchmark for question answering research. *Transactions of the Association for Computational Linguistics*, 7:452–466, 2019. doi: 10.1162/tacl\_a\_00276. URL https://aclanthology.org/Q19-1026.

Guokun Lai, Qizhe Xie, Hanxiao Liu, Yiming Yang, and Eduard H. Hovy. Race: Large-scale reading comprehension dataset from examinations. In *Conference on Empirical Methods in Natural Language Processing*, 2017. URL https://api.semanticscholar.org/CorpusID:6826032.

- Guillaume Lample, Alexandre Sablayrolles, Marc'Aurelio Ranzato, Ludovic Denoyer, and Hervé Jégou. Large memory layers with product keys. *Advances in Neural Information Processing Systems*, 32, 2019.
- Kyungsu Lee, Jaeseung Yang, Haeyun Lee, and Jae Youn Hwang. Stochastic adaptive activation function. In *Proceedings of the 36th International Conference on Neural Information Processing Systems*, NIPS '22, Red Hook, NY, USA, 2022. Curran Associates Inc. ISBN 9781713871088.
- Jiawei Liu, Chunqiu Steven Xia, Yuyao Wang, and Lingming Zhang. Is your code generated by chatGPT really correct? rigorous evaluation of large language models for code generation. In *Thirty-seventh Conference on Neural Information Processing Systems*, 2023. URL https://openreview.net/forum?id=1qvx610Cu7.
- Ilya Loshchilov and Frank Hutter. Decoupled weight decay regularization. In *International Conference on Learning Representations*, 2017. URL https://api.semanticscholar.org/CorpusID:53592270.
- Andrew L Maas, Awni Y Hannun, Andrew Y Ng, et al. Rectifier nonlinearities improve neural network acoustic models. In *Proc. icml*, volume 30, pp. 3. Atlanta, GA, 2013.
- Todor Mihaylov, Peter Clark, Tushar Khot, and Ashish Sabharwal. Can a suit of armor conduct electricity? a new dataset for open book question answering. In Ellen Riloff, David Chiang, Julia Hockenmaier, and Jun'ichi Tsujii (eds.), *Proceedings of the 2018 Conference on Empirical Methods in Natural Language Processing*, pp. 2381–2391, Brussels, Belgium, October-November 2018. Association for Computational Linguistics. doi: 10.18653/v1/D18-1260. URL https://aclanthology.org/D18-1260/.
- Siyuan Mu and Sen Lin. A comprehensive survey of mixture-of-experts: Algorithms, theory, and applications, 03 2025.
- Prajit Ramachandran, Barret Zoph, and Quoc V. Le. Searching for activation functions. ArXiv, abs/1710.05941, 2018. URL https://api.semanticscholar.org/CorpusID: 10919244.
- Joseph Redmon, Santosh Kumar Divvala, Ross B. Girshick, and Ali Farhadi. You only look once: Unified, real-time object detection. 2016 IEEE Conference on Computer Vision and Pattern Recognition (CVPR), pp. 779-788, 2015. URL https://api.semanticscholar.org/CorpusID:206594738.
- Tal Ridnik, Hussam Lawen, Asaf Noy, Emanuel Ben, Baruch Gilad Sharir, and Itamar Friedman. Tresnet: High performance gpu-dedicated architecture. In 2021 IEEE Winter Conference on Applications of Computer Vision (WACV), pp. 1399–1408, 2021. doi: 10.1109/WACV48630.2021.00144.
- Keisuke Sakaguchi, Ronan Le Bras, Chandra Bhagavatula, and Yejin Choi. Winogrande: An adversarial winograd schema challenge at scale. *Proceedings of the AAAI Conference on Artificial Intelligence*, 34(05):8732-8740, Apr. 2020. doi: 10.1609/aaai.v34i05.6399. URL https://ojs.aaai.org/index.php/AAAI/article/view/6399.
- Noam M. Shazeer. Glu variants improve transformer. ArXiv, abs/2002.05202, 2020. URL https://api.semanticscholar.org/CorpusID:211096588.
- Nitish Srivastava, Geoffrey Hinton, Alex Krizhevsky, Ilya Sutskever, and Ruslan Salakhutdinov. Dropout: a simple way to prevent neural networks from overfitting. *The journal of machine learning research*, 15(1):1929–1958, 2014.

Jianlin Su, Yu Lu, Shengfeng Pan, Bo Wen, and Yunfeng Liu. Roformer: Enhanced transformer with rotary position embedding. *ArXiv*, abs/2104.09864, 2021. URL https://api.semanticscholar.org/CorpusID:233307138.

Hugo Touvron, Thibaut Lavril, Gautier Izacard, Xavier Martinet, Marie-Anne Lachaux, Timothée Lacroix, Baptiste Rozière, Naman Goyal, Eric Hambro, Faisal Azhar, Aur'elien Rodriguez, Armand Joulin, Edouard Grave, and Guillaume Lample. Llama: Open and efficient foundation language models. ArXiv, abs/2302.13971, 2023. URL https://api.semanticscholar.org/CorpusID:257219404.

Ashish Vaswani, Noam M. Shazeer, Niki Parmar, Jakob Uszkoreit, Llion Jones, Aidan N. Gomez, Lukasz Kaiser, and Illia Polosukhin. Attention is all you need. In *Neural Information Processing Systems*, 2017. URL https://api.semanticscholar.org/CorpusID: 13756489.

Tianwen Wei, Bo Zhu, Liang Zhao, Cheng Cheng, Biye Li, Weiwei Lü, Peng Cheng, Jianhao Zhang, Xiaoyu Zhang, Liang Zeng, Xiaokun Wang, Yutuan Ma, Rui Hu, Shuicheng Yan, Han Fang, and Yahui Zhou. Skywork-moe: A deep dive into training techniques for mixture-of-experts language models, 2024. URL https://arxiv.org/abs/2406.06563.

Qwen An Yang, Baosong Yang, Beichen Zhang, Binyuan Hui, Bo Zheng, Bowen Yu, Chengyuan Li, Dayiheng Liu, Fei Huang, Guanting Dong, Haoran Wei, Huan Lin, Jian Yang, Jianhong Tu, Jianwei Zhang, Jianxin Yang, Jiaxin Yang, Jingren Zhou, Junyang Lin, Kai Dang, Keming Lu, Keqin Bao, Kexin Yang, Le Yu, Mei Li, Mingfeng Xue, Pei Zhang, Qin Zhu, Rui Men, Runji Lin, Tianhao Li, Tingyu Xia, Xingzhang Ren, Xuancheng Ren, Yang Fan, Yang Su, Yi-Chao Zhang, Yunyang Wan, Yuqi Liu, Zeyu Cui, Zhenru Zhang, Zihan Qiu, Shanghaoran Quan, and Zekun Wang. Qwen2.5 technical report. ArXiv, abs/2412.15115, 2024. URL https://api.semanticscholar.org/CorpusID:274859421.

Rowan Zellers, Ari Holtzman, Yonatan Bisk, Ali Farhadi, and Yejin Choi. Hellaswag: Can a machine really finish your sentence? In *Annual Meeting of the Association for Computational Linguistics*, 2019. URL https://api.semanticscholar.org/CorpusID: 159041722.

Biao Zhang and Rico Sennrich. Root mean square layer normalization. ArXiv, abs/1910.07467, 2019. URL https://api.semanticscholar.org/CorpusID:113405151.

# 

# 

## 

## 

# 

### 

# 

# 

# 

# APPENDIX

### Architecture detail

Parameter	LM1.5B	LM3B
Number of parameters	1.5B	3B
Layers	28	36
Hidden dimension	1536	2048
Intermediate dimension	8960	11008
Number of attention heads	12	16
Number of key-value heads	2	2

Table 4: LM1.5B and LM3B model parameters

### Sparsity Analysis

In Table 5, we report the sparsity rates resulting from the gating in the FFN layer, when using the following activations: RELU, SILU, Swi+FT fine-tuning, and when using StochA with Swi+FT for varying values p. In all cases except for the SILU baseline, we use RELU at test time.

	train	inference	Swi+FT	StochA: p	Swi+FT: $\alpha$	sparsity (%)
baselines	SILU RELU	SILU RELU				0.0002 94.8
Swi+FT	SILU	RELU	✓		0.05	79.9
StochA +Swi+FT	[S R]-S+ [S R]-S+ [S R]-S+	RELU RELU RELU	√ √ √	0.3 0.5 0.7	$0.05 \\ 0.05 \\ 0.05$	88.5 86.5 84.6

Table 5: Sparsity analysis: We plot the rate of the 0-valued activation after the SILU (not sparse) and RELU activation, when training with the LM1.5B model with standard SILU and RELU. The Swi+FT fine-tuning with RELU brings back a lot of sparsity (80%), yet the model is not competitive. The combination of StochA with Swi+FT leads to models offering a high sparsity degree by using RELU at test time and at the same time with competitive performance, see Tables 1 and 2.

### $\mathbf{C}$ BENCHMARKS

Code generation We use two benchmarks that evaluate the code generation capabilities of AI models: HumanEval+ and MBPP.

- The HumanEval+ (Liu et al., 2023) benchmark is an extension of HumanEval (Chen et al., 2021), which is designed to evaluate the functional correctness of code generated by AI models.
- MBPP (Austin et al., 2021) is designed to evaluate the code generation abilities of AI models, particularly for Python programming tasks.

Common sense and general reasoning We use benchmarks consisting of questionanswer or multiple-choice questions designed to evaluate the commonsense reasoning abilities of AI models, particularly in the context of natural language understanding: HellaSWAG, ARC, PIQA, OBQA, Winogrande, NaturalQuestions, RACE, TQA and GSM8K.

• HellaSWAG (Zellers et al., 2019) consists of multiple-choice questions where each question contains a short context (a sentence or paragraph) followed by four possible continuations. Only one continuation is correct and makes sense given the context. • The AI Reasoning Challenge (ARC) (Clark et al., 2018) benchmark consists of multiple-choice science questions typically found in elementary and middle school exams. The ARC questions require a mix of factual knowledge, commonsense reasoning, and multi-step inference.

- The Physical Interaction Question-Answering (PIQA) (Bisk et al., 2020) benchmark consists of multiple-choice questions about how to accomplish simple physical tasks. Each question presents a short scenario and two possible solutions; only one is physically plausible.
- The OpenBook QA (OBQA) (Mihaylov et al., 2018) benchmark consists of 6,000 multiple-choice questions based on elementary science facts. Each question is designed to require combining a provided "open book" science fact with additional commonsense or general knowledge.
- WinoGrande (Sakaguchi et al., 2020) benchmark consists of multiple-choice questions. Each question presents a sentence with a pronoun and two possible antecedents; the task is to choose the correct referent for the pronoun.
- Natural Questions (NQ) (Kwiatkowski et al., 2019) benchmark is designed to evaluate the ability of an AI model to answer real user questions using information from Wikipedia.
- The Reading Comprehension from Examinations (RACE) (Lai et al., 2017) benchmark consists of passages and multiple-choice questions to assess how well AI models can comprehend and reason about written passages.
- The Trivia QA benchmark (TQA) (Joshi et al., 2017) is a reading comprehension dataset that pairs trivia questions with evidence documents from which answers can be derived.
- The Grade School Math 8k (GSM8k) (Cobbe et al., 2021) benchmark is a dataset of 8,500 high-quality, linguistically diverse grade school math word problems. The benchmark is designed to test multi-step mathematical reasoning capabilities in language models.

Benchmark	Metric	Few Shot	Type
hellaswag	acc_char	0	choice
winogrande	$acc\_char$	0	choice
arc_easy	$acc\_char$	0	choice
arc_challenge	$acc\_char$	0	choice
piqa	$\operatorname{acc\_char}$	0	choice
obqa	$acc\_char$	0	choice
race.middle	$acc\_char$	0	choice
race.high	$acc\_char$	0	choice
human_eval_plus	pass@1	0	generation
mbpp	compiles@1	3	generation
tqa	f1	5	generation
nq	f1	5	generation

Table 6: We few-shot prompt the LM1.5B and LM3B models and the given metric per benchmark as well as the average performance.

### D Examples of various sequences generated with StochA

Using a pre-trained LM3B model with StochA, we can use the StochA activation at test time to generate multiple predictions by leveraging the randomness from the activation function. We provide two examples of the generations obtained using questions from the TQA benchmark (Joshi et al., 2017):

question and accepted answers	generated answers	number of times	NLL score	Scor
	1988	4	1.002	
When did ibuprofen become	1982	11	1.004	
available over the counter?	1980	1	1.030	
A: 1983	1995	2	1.019	
A: 1984	2001	1	1.017	
	1983	1	1.024	
Who played michael jackson	Michael Jackson	19	0.948	
in jackson 5 movie?	Michael jackson	1	0.792	
A:alex burrall				
A:abolade david olatunde				
A:wylie draper				
A:jason weaver				
Where is the meridian that	Greenwich	9	0.896	
is opposite the prime	Greenwich, England	11	0.551	
meridian located?				
A:180th meridian				
A:antimeridian				
The cold dry winds that	Siberian	7	1.099	
blow over northern india in	Siberian winds	6	0.970	
winter are called?	Ganges	1	1.617	
A:northeast monsoon	monsoon	2	1.051	2,
A:retreating monsoon	katabatic winds	3	0.738	
A:northeast monsoon or	Ganga	1	1.643	
retreating monsoon				
W/l :	Blood	6	1.262	
Where can you find dna in the body?	Hair	12	1.393	
A:chromosomes in cell	Mitochondria	1	0.700	
A:inside cell nucleus	In the nucleus	1	1.437	2,
Timble cen nucleus				
Who is often associated	Johannes Gutenberg	20	0.205	
with printing the first book				
using moveable type in				
germany?				
A:johannes gutenberg				
Who won the womens 2017	Kentucky	15	1.852	
ncaa basketball	Kentucky Wildcats	1	1.304	
	North Carolina	4	1.342	1,
tournament/				
A:south carolina	USA	14	0.818	
A:south carolina  Country with most olympic	USA United States	14 6	0.818 0.614	
A:south carolina  Country with most olympic gold medals all time?				
A:south carolina  Country with most olympic gold medals all time?	United States	6	0.614	
A:south carolina  Country with most olympic gold medals all time?  A:united states	United States	14	0.614	
A:south carolina  Country with most olympic gold medals all time?  A:united states  The atomic number of	United States  5 49	6 14 5	0.614 0.579 0.650	
A:south carolina  Country with most olympic gold medals all time?  A:united states  The atomic number of indium which belongs to	United States	14	0.614	
A:south carolina  Country with most olympic gold medals all time?  A:united states  The atomic number of indium which belongs to 5th period is?	United States  5 49	6 14 5	0.614 0.579 0.650	
A:south carolina  Country with most olympic gold medals all time?  A:united states  The atomic number of indium which belongs to 5th period is?	United States  5 49 84	14 5 1	0.614 0.579 0.650 0.695	
A:south carolina  Country with most olympic gold medals all time? A:united states  The atomic number of indium which belongs to 5th period is? A:49	United States  5 49 84  The president	14 5 1	0.614 0.579 0.650 0.695	
A:south carolina  Country with most olympic gold medals all time? A:united states  The atomic number of indium which belongs to 5th period is? A:49  Who appoints the members	United States  5 49 84	14 5 1	0.614 0.579 0.650 0.695	2
A:south carolina  Country with most olympic gold medals all time? A:united states  The atomic number of indium which belongs to 5th period is? A:49  Who appoints the members of the board of governors of	United States  5 49 84  The president	14 5 1	0.614 0.579 0.650 0.695	2,
Country with most olympic gold medals all time? A:united states The atomic number of indium which belongs to 5th period is? A:49 Who appoints the members of the board of governors of the federal reserve? A:president	United States  5 49 84  The president The president of the United States	14 5 1 16 4	0.614 0.579 0.650 0.695 0.602 0.431	2,
A:south carolina  Country with most olympic gold medals all time? A:united states  The atomic number of indium which belongs to 5th period is? A:49  Who appoints the members of the board of governors of the federal reserve? A:president	United States  5 49 84  The president The president of the United States	14 5 1 16 4	0.614 0.579 0.650 0.695 0.602 0.431	2,
A:south carolina  Country with most olympic gold medals all time? A:united states  The atomic number of indium which belongs to 5th period is? A:49  Who appoints the members of the board of governors of the federal reserve? A:president  What age do you need to be	United States  5 49 84  The president The president of the United States	14 5 1 16 4	0.614 0.579 0.650 0.695 0.602 0.431 0.660 0.680	2,
A:south carolina  Country with most olympic gold medals all time? A:united states  The atomic number of indium which belongs to 5th period is? A:49  Who appoints the members of the board of governors of the federal reserve? A:president.  What age do you need to be to buy a bb gun?	United States  5 49 84  The president The president of the United States	14 5 1 16 4	0.614 0.579 0.650 0.695 0.602 0.431	2,
A:south carolina  Country with most olympic gold medals all time? A:united states  The atomic number of indium which belongs to 5th period is? A:49  Who appoints the members of the board of governors of the federal reserve?	United States  5 49 84  The president The president of the United States  14 10 18	14 5 1 16 4 17 2 1	0.614 0.579 0.650 0.695 0.602 0.431 0.660 0.680 0.728	
A:south carolina  Country with most olympic gold medals all time? A:united states  The atomic number of indium which belongs to 5th period is? A:49  Who appoints the members of the board of governors of the federal reserve? A:president  What age do you need to be to buy a bb gun? A:18	United States  5 49 84  The president of the United States  14 10 18  Fantasy	14 5 1 16 4 17 2 1	0.614 0.579 0.650 0.695 0.602 0.431 0.660 0.680 0.728 1.038	1,
A:south carolina  Country with most olympic gold medals all time? A:united states  The atomic number of indium which belongs to 5th period is? A:49  Who appoints the members of the board of governors of the federal reserve? A:president  What age do you need to be to buy a bb gun? A:18  What genre is the magic	United States  5 49 84  The president The president of the United States  14 10 18  Fantasy Children's fiction	14 5 1 16 4 17 2 1	0.614 0.579 0.650 0.695 0.602 0.431 0.660 0.680 0.728 1.038 1.051	1,2
A:south carolina  Country with most olympic gold medals all time? A:united states  The atomic number of indium which belongs to 5th period is? A:49  Who appoints the members of the board of governors of the federal reserve? A:president  What age do you need to be to buy a bb gun? A:18  What genre is the magic tree house books?	United States  5 49 84  The president The president of the United States  14 10 18  Fantasy Children's fiction Children's	14 5 1 16 4 17 2 1 1 14 1 1 3	0.614 0.579 0.650 0.695 0.602 0.431 0.660 0.680 0.728 1.038 1.051 1.245	1, 2, 1, 1, 1, 1, 1, 1, 1, 1, 1, 1, 1, 1, 1,
A:south carolina  Country with most olympic gold medals all time? A:united states  The atomic number of indium which belongs to 5th period is? A:49  Who appoints the members of the board of governors of the federal reserve? A:president  What age do you need to be to buy a bb gun? A:18  What genre is the magic tree house books?	United States  5 49 84  The president The president of the United States  14 10 18  Fantasy Children's fiction	14 5 1 16 4 17 2 1	0.614 0.579 0.650 0.695 0.602 0.431 0.660 0.680 0.728 1.038 1.051	1, 2, 1, 1, 1, 1, 1, 1, 1, 1, 1, 1, 1, 1, 1,
A:south carolina  Country with most olympic gold medals all time? A:united states  The atomic number of indium which belongs to 5th period is? A:49  Who appoints the members of the board of governors of the federal reserve? A:president  What age do you need to be to buy a bb gun? A:18  What genre is the magic tree house books?	United States  5 49 84  The president The president of the United States  14 10 18  Fantasy Children's fiction Children's Children's books	14 5 1 16 4 17 2 1 1 14 1 3 2	0.614 0.579 0.650 0.695 0.602 0.431 0.660 0.680 0.728 1.038 1.051 1.245 1.067	1, 2, 1, 1, 1, 1, 1, 1, 1, 1, 1, 1, 1, 1, 1,
A:south carolina  Country with most olympic gold medals all time? A:united states  The atomic number of indium which belongs to 5th period is? A:49  Who appoints the members of the board of governors of the federal reserve? A:president.  What age do you need to be to buy a bb gun?	United States  5 49 84  The president The president of the United States  14 10 18  Fantasy Children's fiction Children's Children's Children's	14 5 1 16 4 17 2 1 14 13 2	0.614 0.579 0.650 0.695 0.602 0.431 0.660 0.680 0.728 1.038 1.051 1.245 1.067	2, 1, 2, 1, 2,
A:south carolina  Country with most olympic gold medals all time? A:united states  The atomic number of indium which belongs to 5th period is? A:49  Who appoints the members of the board of governors of the federal reserve? A:president  What age do you need to be to buy a bb gun? A:18  What genre is the magic tree house books? A:childrens historical fantasy	United States  5 49 84  The president The president of the United States  14 10 18  Fantasy Children's fiction Children's Children's books	14 5 1 16 4 17 2 1 1 14 1 3 2	0.614 0.579 0.650 0.695 0.602 0.431 0.660 0.680 0.728 1.038 1.051 1.245 1.067	1, 2, 1, 1, 1, 1, 1, 1, 1, 1, 1, 1, 1, 1, 1,

Table 7: Example generations. For each question, we indicate the ground-truth answers (from the dataset). We generate 20 answers per question with [S|R]-S+, p=0.7. We list the de-duplicated answers, with the NLL score (used to sort the results) and the F1 score (used to evaluate the result, it is computed as the intersection of bags-of-words).